SAND2015-9244C

A Numerical Round Robin for the Prediction of the Dynamics of Jointed Structures

J. Gross[(a)], J. Armand[(b)], R.M. Lacayo[(c)], P. Reuss[(a)], L. Salles[(b)], C.W. Schwingshackl[(b)], M.R.W. Brake[(c)], R.J. Kuether[(c)]

[(a)] University of Stuttgart, Institute of Applied and Experimental Mechanics, Stuttgart, Germany
[(b)] Imperial College London, Mechanical Engineering, London, UK
[(c)] Sandia National Laboratories[1], Component Science and Mechanics, Albuquerque, NM, USA

ABSTRACT
Motivated by the current demands in high-performance structural analysis, and by a desire to better model systems with localized nonlinearities, analysts have developed a number of different approaches for modelling and simulating the dynamics of a bolted-joint structure. However, the types of conditions that make one approach more effective than the others remains poorly understood due to the fact that these approaches are developed from fundamentally and phenomenologically different concepts. To better grasp their similarities and differences, this research presents a numerical round robin that assesses how well three different approaches predict and simulate a mechanical joint. These approaches are applied to analyze a system comprised of two linear beam structures with a bolted joint interface, and their strengths and shortcomings are assessed in order to determine the optimal conditions for their use.

KEYWORDS: nonlinear damping; nonlinear vibration; bolted joint; finite element analysis; harmonic balance.

1. INTRODUCTION

A large number of systems that many structural dynamics engineers study are composed of two or more elastic components that are mechanically joined together, such as through a bolted lap joint. To predict the dynamics and vibration of such systems, analysts typically develop linear finite element models for each component separately, and then couple the components with nonlinear models that are localized to the region of the joint. With current methods, analysts are very good at creating predictive models for the individual components. However, a general process to account for the contribution of the joint in the dynamics of the system has yet to be established fully. Fortunately, researchers in recent years have developed a number of different approaches for modelling joints in specific systems. This research attempts to apply and compare the methods used in three different approaches on a recognized benchmark system in order to gain insight on the best practices for modelling joints.

This research is a product of the numerical round robin project from the 2015 Nonlinear Mechanics and Dynamics (NOMAD) Summer Research Institute hosted by Sandia National Laboratories, and is a continuation of the research done under the same project during the 2014 NOMAD Institute [1]. The objective for the 2015 numerical round robin is largely the same in that the authors seek a better understanding of the capabilities for different approaches to model the nonlinear dynamic behaviour of bolted joints. This round robin project examines three different nonlinear response prediction methods developed respectively at the Vibration University Technology Centre at Imperial College London (hereafter referred to as Imperial), the Component Science and Mechanics Center at Sandia National Laboratories (referred to as Sandia), and the Institute of Applied and Experimental Mechanics at the University of Stuttgart (referred to as Stuttgart). The three methods are applied to model a bolted lap joint in a straight beam (Brake-Reuss beam) benchmark structure, and their simulated nonlinear dynamic responses are used as the basis for comparison.

More so than in the 2014 project, the 2015 round robin project emphasized modelling the Brake-Reuss beam more realistically. For example, the 2015 beam includes a model for the bolts, and uses advanced modelling techniques for incorporating bolt pre-tension. In addition, boundary conditions are prescribed based on performed experiments. Furthermore, this work presents new insights into the differences between the methods, and new ways of comparing their predictions in terms of the changes in the modal natural frequency and damping with forcing/response amplitude., A single-degree of freedom system was studied to shed light onto the different model parameters (slip force, tangential stiffness, etc.) used in

[1] Sandia National Laboratories is a multi-program laboratory managed and operated by Sandia Corporation, a wholly owned subsidiary of Lockheed Martin Corporations, for the U.S. Department of Energy's National Nuclear Security Administration under Contract DE-AC04-94AL85000.

each method and on the physics that they capture. This research practices all these methods in preparation for a future validation study with experimental data.

2. THE BENCHMARK MODEL

The test case chosen for the round robin investigation is the Brake-Reuss beam [2], a structure consisting of two identical straight beams connected with a lap joint (see Fig. 1). The beams are made of stainless steel alloy 304, and have an assembled dimension of 28.38×1×1 inches. In the middle of the structure, the two component beams have half-width extensions, which overlap each other to form the lap joint while preserving the prismatic shape of the entire structure. The lap joint contains three through-holes along its length that allow bolts to clamp the two separate beams together.

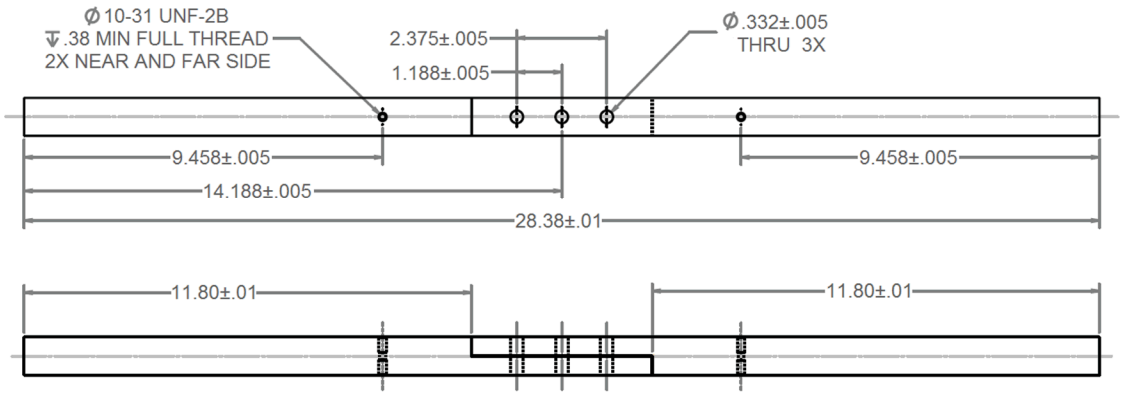

Figure 1: The Brake-Reuss beam and its dimensions (in inches).

2.1. The finite element mesh

A linear finite element model of the Brake-Reuss beam, depicted in Fig. 2, is built in Abaqus and used in all three approaches. Each beam is composed of 8240 8-node hexahedral elements, along with 340 6-node wedge elements on account of the shape irregularities introduced by the circular lap-joint holes. A particular care has been taken to ensure a matching mesh at the contact interface between the two beams to allow the option to couple the coincident nodes between the two surfaces with a nonlinear contact element. The interface mesh, shown in Fig. 3, contains 592 nodes, so up to 592 nonlinear contact elements may be used for analysis.

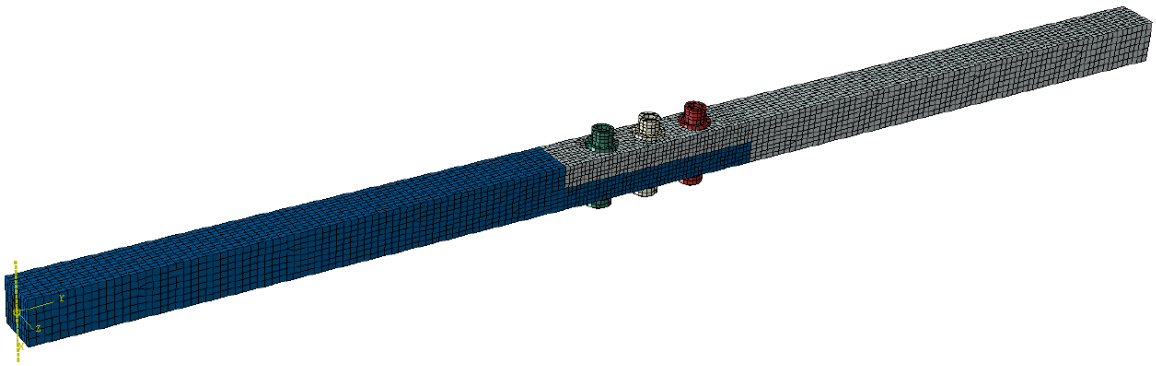

Figure 2: Finite element model of the Brake-Reuss beam.

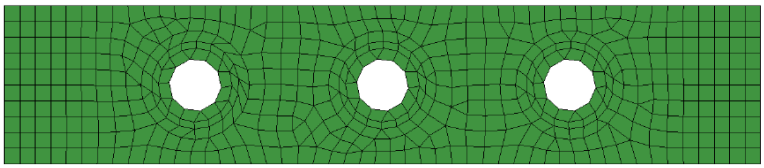

Figure 3: Contact interface mesh.

The beam finite element model includes the three bolts at the lap-joint. Each bolt assembly contains a bolt, a nut, and two washers, which are all modelled as a single, solid mesh. The bolt meshes are uncoupled from the rest of the beam structure except at the interface between the washers and the top and bottom surfaces of the beams where fixed coupling is applied.

In all subsequent analyses, both the beams and bolts use an isotropic, elastic material model with Young's modulus $E =$ 189768 N/mm^2, Poisson's ratio $\nu = 0.32$, and mass density $\rho = 7.82\times10^{-6}$ kg/mm^3. The structure is given fixed-free boundary conditions, where the square surface on the left extremity of the beam in Fig. 2 is fixed.

3. NONLINEAR STATIC ANALYSIS

A non-linear static analysis is performed on the bolted structure to determine the pressure distribution at the contact interface between the two beams.

The pre-tensioning of the bolts is applied by using the 'bolt load' feature available in Abaqus. The shaft of the bolt is cut at mid-length through a pre-tension section, and the prescribed force is applied to this section along the axis of the bolt, as illustrated in Fig. 4. A surface-to-surface approach with a direct enforcement method (based on Lagrange multipliers) is used to solve the contact problem. A penalty method formulation with a friction coefficient $\mu = 0.6$ is used to describe the frictional behaviour.

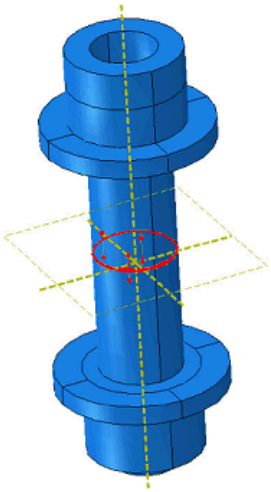

Figure 4: Bolt pre-tensioning.

Figure 5(a) shows the obtained pressure distribution for an applied pre-tension load of 4 kN. As expected, the pressure is maximum around the bolt holes and reduces concentrically leading to an area of lower compression between the holes. There is a nil pressure near both ends of the contact interface, which is due to a small gap opening that can be observed Fig. 5(b). The pressure results of the nonlinear static analysis are used as a starting point to generate the nonlinear dynamic models, as will be explained subsequently.

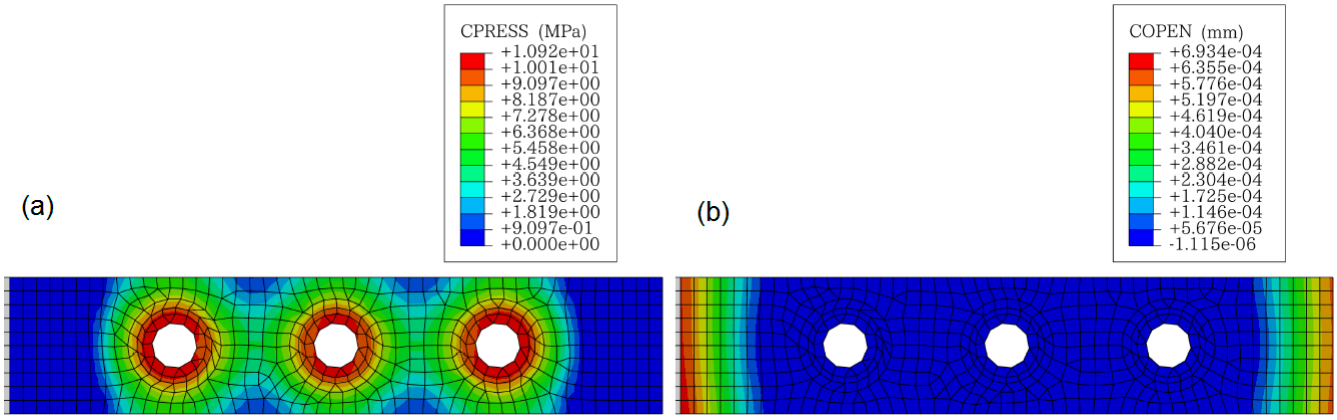

Figure 5: (a) The calculated contact pressure and (b) gap spacing in the contact interface.

4. CONSIDERED APPROACHES TO MODELLING FRICTION JOINTS

The Brake-Reuss beam benchmark system defined in Section 2 is tested with three different joint-modelling approaches as developed respectively by the three contributing institutions: Sandia, Stuttgart, and Imperial. The major differences between the three approaches are summarized in Table 1.

Table 1: Summary of Considered Approaches for Modelling Joints.

	Sandia Approach	Stuttgart Approach	Imperial Approach
Finite Element Tool	SIERRA/SD	CalculiX	NASTRAN
Model Fidelity	Craig-Bampton ROM or Full FE Model	Craig-Bampton ROM	Hybrid ROM
Nonlinear Element	Iwan Element	Jenkins Element	3D Contact Element
Solver Type	Time Integrator	Single-Harmonic Balance	Multi-Harmonic Balance

Each approach is explained in more detail in the subsections that follow, but a general comment must be made about the response output that each nonlinear solver produces. The responses for the methods developed at Sandia are obtained in the time domain, whereas Stuttgart and Imperial both use harmonic balance methods (HBM) to obtain responses in the frequency domain. The Sandia transient methods are versatile in that they are developed for arbitrary excitations and nonlinear constitutive models, but they become very expensive if the steady state frequency response is desired (because one would have to integrate the response from some initial condition until steady state is reached). In contrast, the Stuttgart and Imperial HBM can compute the steady-state response in a computationally efficient manner, but are not currently capable of computing the transient response of the structure. The two HBM approaches differ mainly in the implementation of the nonlinear forces (linearization for Stuttgart versus alternating frequency-time procedure for Imperial). These differences will need to be kept in mind when evaluating the resulting responses of the beam. In general, transient response methods are not easily comparable to frequency response methods, but this work has exploited the similarity between the resonant response of a nonlinear structure and the response to a slowly decaying transient to make a meaningful comparison, as will be explained subsequently.

4.1. Sandia Approach

Over the past few decades, Sandia pioneered an approach in which a joint is replaced with a "whole joint element," such as Segalman's four-parameter Iwan element [3], which is able to capture the amplitude-dependent energy dissipation and stiffness of the joint. In general, an Iwan element, as seen in Fig. 6(a), is a one-dimensional model consisting of an infinite number of friction sliders (Jenkins elements) in parallel whose slip force strengths follow a certain distribution [4]. The four-parameter formulation assumes a power-law distribution ending with a Dirac delta function at maximum slip strength (see Fig

6(b)). Such a distribution produces a joint whose energy dissipation per cycle follows a power-law relationship with the joint excitation force (shown in Fig. 6(c)), a phenomenon that has been observed experimentally in several structures [5,6]. The four parameters for this Iwan element formulation are the joint force at the inception of macro-slip (typically denoted as F_S), the tangent stiffness in microslip (K_T), the power-law slope of energy dissipation (χ), and the ratio (β) of the Dirac delta function (associated with macro-slip) to the power-law term (associated with micro-slip). The Iwan model has been well-validated at least within joint micro-slip regimes [3,6-8].

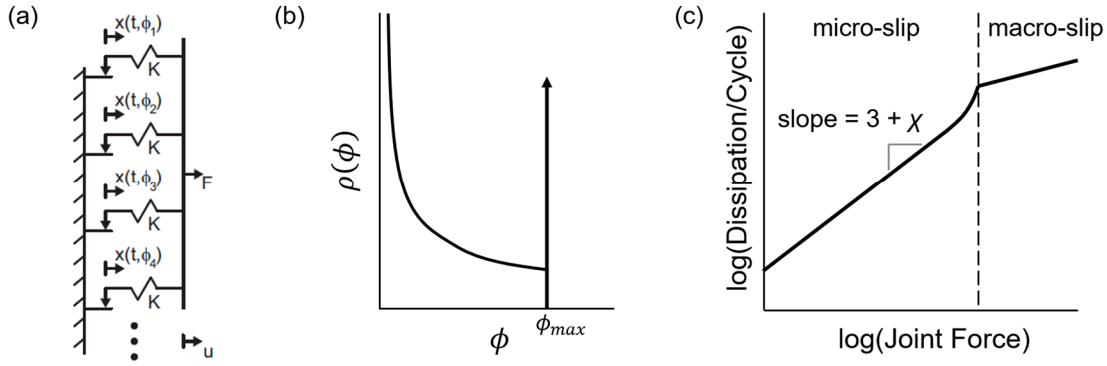

Figure 6: (a) A parallel-series Iwan element, (b) the population density function ρ for sliders with slip strength ϕ in the four-parameter formulation of the Iwan element, and (c) the resulting power-law relationship between energy dissipation per cycle and joint force.

It should be noted that the Iwan model was not developed to predict the response of a single joint, but to represent a joint with known properties in a larger structural model. In contrast, the approaches developed at Imperial and Stuttgart predict the response of a single joint, by assuming that a Coulomb friction model holds at the interface. The four-parameter Iwan model is designed to reproduce the power-law energy dissipation vs. joint force behaviour observed in experimental tests on the hardware of interest [6]. As such, the parameters for the Iwan element can only be tuned after measurements have been made or based on high fidelity simulations of the interface mechanics. Hence, the Iwan model is not perfectly comparable to the other two approaches. On the other hand, the Iwan model is known to exhibit the power-law behaviour that is observed in many jointed structures, whereas it is not yet clear whether the other formulations will predict power-law behaviour or how that behaviour will relate to their input parameters.

Since the intent of an Iwan element is to use a single element to represent the joint as a whole, only one Iwan element is typically used to represent an interface, which may in fact contain some microscopic regions that are stuck and others that are sliding. In the context of finite elements, an Iwan element should not be used to couple individually all coincident nodes between the two interfacing surfaces. Rather, the state of all nodes on a friction surface should contribute to the state of the Iwan element. This can be done in practice by creating a virtual node to represent the surface, and then tying all the physical nodes to the virtual node with rigid bar elements or with an averaging-type multi-point constraint. The two virtual nodes corresponding to the opposite surfaces respectively would then be coupled with the Iwan element.

As was done in previous works, Sandia's in-house finite element solver, SIERRA/SD [9], is used to build the mass and stiffness matrices from the finite element mesh. The matrices are reduced using the Craig-Bampton method [10], and then imported into a structural dynamics solver developed in MATLAB, where the Iwan elements are added to the system. The solver uses an adaptive implicit-explicit numerical integrator [11] to solve the time-domain equations of motion,

$$\mathbf{M}\ddot{\mathbf{q}} + \mathbf{C}\dot{\mathbf{q}} + \mathbf{K}\mathbf{q} = \mathbf{f}_{ext} + \mathbf{f}_{NL}(\mathbf{q}, \dot{\mathbf{q}}, \boldsymbol{\theta}), \tag{1}$$

where $\mathbf{M}$ is the system mass matrix, $\mathbf{K}$ is the stiffness matrix, $\mathbf{C}$ is the matrix of linear material damping coefficients, and $\mathbf{q}$, $\dot{\mathbf{q}}$, and $\ddot{\mathbf{q}}$ are the coordinate displacement, velocity and acceleration response vectors, respectively, for which the integrator solves. The vector $\mathbf{f}_{ext}$ contains the time-dependent external loads applied on the coordinates, and $\mathbf{f}_{NL}$ is the vector of nonlinear forces from the Iwan elements. The vector $\boldsymbol{\theta}$ records a finite number of slider states for each Iwan element, and there are typically 25 to 100 sliders per element.

4.2. Stuttgart Approach

The Stuttgart approach [12] relies on a node-to-node contact model with friction in the tangential direction and a nonlinear contact law in the normal direction. The nonlinear contact law is used to compute the normal force at each node-to-node contact based on the applied loading of the bolts. This is established by the nonlinear static pressure distribution presented in Section 3, which is converted to nodal forces for the dynamic analyses. In subsequent analyses, however, the relative dynamics in the normal direction are supressed, and the normal force at each node in contact is assumed constant for the HBM calculation. In the tangential direction the interface nodes can have relative displacements in two dimensions. Since in this approach only the fundamental response is considered, the resulting motion is an ellipse in the plane of the joint, as seen in Fig. 7(b).

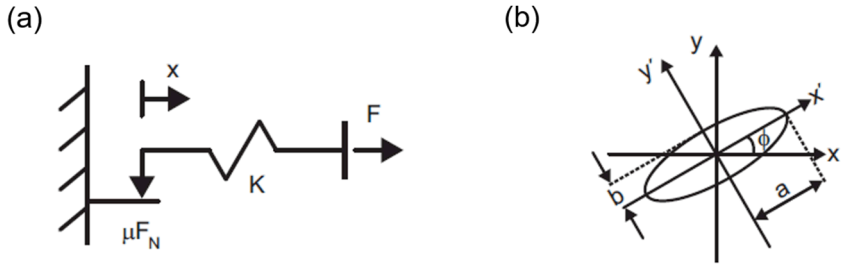

Figure 7: (a) A 2D Jenkins element and (b) the elliptical motion it undergoes in the first harmonic.

The friction forces are then computed for the major and minor axis a and b separately using the analytical equations for the Fourier coefficients [12] in terms of equivalent stiffness and damping of the one dimensional case. This is a further approximation which does not take into account the coupling of the friction force in two dimensions but has been found to produce reasonable results when the motion in one dimension is dominant. In the local coordinate system x' and y', the equivalent stiffness and damping matrix as well as the transformation matrix, including the angle ϕ between the local and the global coordinate system can be written as

$$\mathbf{K}_{hbm}^{l} = \begin{bmatrix} k_{hbm}^{x'} & 0 \\ 0 & k_{hbm}^{y'} \end{bmatrix}, \ \mathbf{D}_{hbm}^{l} = \begin{bmatrix} d_{hbm}^{x'} & 0 \\ 0 & d_{hbm}^{y'} \end{bmatrix}, \ \mathbf{T} = \begin{bmatrix} \cos\phi & \sin\phi \\ -\sin\phi & \cos\phi \end{bmatrix}. \tag{2}$$

Transforming the matrices into the global coordinate system by

$$\mathbf{K}_{hbm}^{g} = \mathbf{T}\mathbf{K}_{hbm}^{l}\mathbf{T}^{T}, \ \mathbf{D}_{hbm}^{g} = \mathbf{T}\mathbf{D}_{hbm}^{l}\mathbf{T}^{T}, \tag{3}$$

a pseudo-receptance matrix in the frequency domain can be established containing the sum of all node-to-node friction contacts by

$$\mathbf{H}_{hbm}(\hat{\mathbf{x}}) = \left(\left(\mathbf{K} + \mathbf{K}_{hbm}(\hat{\mathbf{x}})\right) + i\omega\left(\mathbf{D} + \mathbf{D}_{hbm}(\hat{\mathbf{x}})\right) - \omega^{2}\mathbf{M}\right). \tag{4}$$

The linear mass and stiffness matrices are established by the Craig-Bampton method [10] and hence retain the interface degrees of freedom where the friction forces act.. The resulting equations of motion in the frequency domain can be arranged in an implicit form by

$$\mathbf{r} = \mathbf{H}_{hbm}(\hat{\mathbf{x}})\,\hat{\mathbf{x}} - \mathbf{f}_{ext}. \tag{5}$$

The residual $\boldsymbol{r}$ is then minimised using a Nonlinear Successive Over-Relaxation Method [13] to obtain the nonlinear dynamic response. The advantage of this method is that it avoids having to establish a Jacobian matrix of the equations which is expensive for the large number of considered degrees-of-freedom when using a standard finite-difference method to compute the derivative numerically. On the other hand, this method requires two evaluations of the nonlinear friction forces to compute the Fourier coefficients per iteration step, such that the efficiency of this method in the present case is only guaranteed by fact that the coefficients are computed analytically.

4.3. Imperial approach

The Imperial-developed code, FORSE, used for the analysis of the nonlinear response of flange joints is based on the multi-harmonic representation of the steady-state response and allows large scale realistic friction interface modelling. Major features of the methodology were described in [14] and only an overview of the analysis is presented in this paper. The equation of motion consists of a linear part, which is independent of the vibration amplitudes, and the nonlinear part due to the friction interfaces at the interface joint. The nonlinear equation of motion can be written as

$$\mathbf{K}\mathbf{q}(t) + \mathbf{C}\dot{\mathbf{q}}(t) + \boldsymbol{M}\ddot{\mathbf{q}}(t) + \mathbf{f}\big(\mathbf{q}(t)\big) - \mathbf{p}(t) = \mathbf{0}, \tag{6}$$

where **q** is a vector of displacements; **K**, **C**, and **M** are the stiffness, damping and mass matrices, respectively, of the linear model; **f** is a vector of nonlinear friction interface forces, which is dependent on displacements and velocities of the interacting nodes, and **p** is a vector of periodic exciting forces. The variation of the displacements in time is represented by a restricted Fourier series, which can contain as many harmonic components as it is necessary to approximate the solution, i.e.

$$\mathbf{q}(t) = \mathbf{Q}_0 + \sum_{j=1}^{n} \mathbf{Q}_j^c \cos\big(m_j \omega t\big) + \mathbf{Q}_j^s \sin\big(m_j \omega t\big). \tag{7}$$

In Eq. 9, **Q** are vectors of harmonic coefficients for the system degrees of freedom (DOFs), n is the number of harmonics that is used in the multi-harmonic displacement representation, and ω is the principal vibration frequency. The flowchart of the calculations performed with the code is presented in Fig. 8. The contact interface elements developed in [14] (see Fig. 9) are used for modelling of nonlinear interactions at contact interfaces and analytical expressions for the multi-harmonic representation of the nonlinear contact forces and stiffnesses. The nonlinear algebraic system of the reduced model is obtained using a hybrid method of reduction developed by Petrov [15,16]. The nonlinear system in the frequency domain is

$$\widetilde{\mathbf{Q}} = A(\omega)\big(\tilde{\mathbf{F}} - \tilde{\mathbf{F}}_{nl}(\widetilde{\mathbf{Q}})\big), \tag{8}$$

with $\widetilde{\mathbf{Q}}$ defined as the vector of the Fourier coefficients of the displacements at the interface, $A(\omega)$ the frequency response, $\tilde{\mathbf{F}}$ is the vector of the Fourier coefficients of the excitation force and $\tilde{\mathbf{F}}_{nl}$ is the vector of the Fourier coefficients of the nonlinear contact forces.

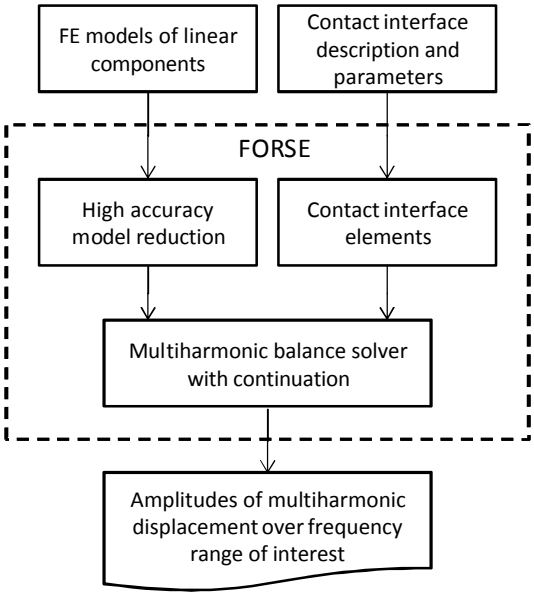

Figure 8: The scheme of the forced response analysis

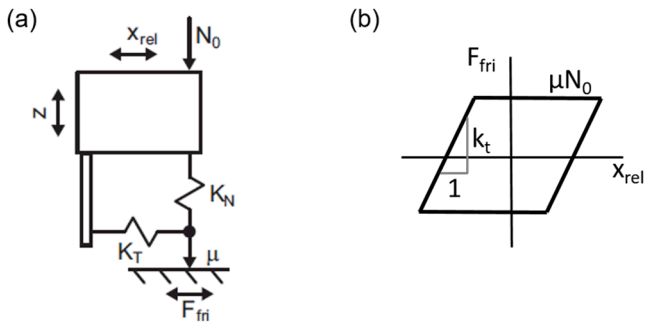

Figure 9: (a) The 3D contact element and (b) its approximate hysteresis curve.

5. SDOF COMPARISON BETWEEN NONLINEAR ELEMENTS

An Iwan element is a collection of parallel Jenkins elements, so one would expect it to produce joint behaviour similar to the Jenkins and 3D contact elements. However, the latter elements assume a Coulomb friction formulation, where the energy dissipated can be predicted after deriving the slip force based on the normal contact pressure. In contrast, the four-parameter Iwan element used in this work is formulated a priori to produce a power-law relationship between energy dissipation and the force, based on experiments that were reported in [6]. These different formulations make it difficult to gauge, relative to each other, how each element will dissipate energy within a structure. In order to clarify the similarities and differences between these elements, a study is conducted to compare how each element dampens the motion of the single-degree of freedom (SDOF) system in Fig. 10. This will also illustrate the extent to which the models can be tuned to give similar dynamic responses.

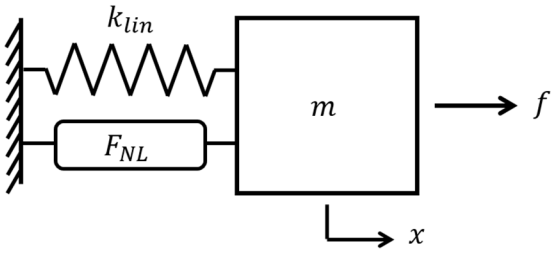

Figure 10: A single-degree of freedom system used in the comparison study. The system contains a single mass, $\boldsymbol{m}$, connected to ground with a linear spring of stiffness $\boldsymbol{k_{lin}}$ and a nonlinear element applying reaction force $\boldsymbol{F_{NL}}$ on the mass.

The two parameters for the Jenkins element are the slip force, which is set to a value of 100 N, and the tangent stiffness, which is set to a value of 3000 N/mm. The mass in the system is set to be unitary, and a value of 40,000 N/mm is chosen for the stiffness of the linear spring so that the natural frequency for the linear system matches that of the first bending mode for the fixed-free Brake-Reuss beam (approximately 31 Hz).

5.1. How Each Approach Calculates Damping

Each of the three considered approaches calculates the equivalent damping using different methods. Stuttgart's harmonic balance method calculates the amplitude-dependent nonlinear force from the Jenkins element at every frequency, and represents that force with equivalent damping and stiffness values. The phase plot of the frequency response was used to determine the frequency where the displacement phase lags that of the input force by 90° (resonance), then the damping coefficient was extracted at that same frequency.

Imperial's method solves for the frequency-domain tangential force and displacement at resonance. The inverse discrete Fourier transform is then applied to the solution to obtain the time histories for force and displacement over one cycle at

resonance. The time histories are used to construct a hysteresis curve, the area of which is the energy dissipated in that cycle. The energy dissipation is converted to an equivalent damping using the following equation derived in [8],

$$\zeta_r = \frac{D_r}{2\pi|V_r|^2}, \tag{9}$$

where D is the energy dissipated per cycle at resonance and ζ_r is the equivalent critical damping ratio near the resonance mode of interest. In a single-degree of freedom system with unit mass, $|V_r|$ is the peak velocity of the mass at resonance. Otherwise, $|V_r|$ is the velocity of the mass-normalized modal coordinate corresponding to the resonance mode of interest.

While the Jenkins and 3D contact elements rely on harmonic balance methods to compute the steady state response, Iwan elements are typically simulated in the time domain. One could reconcile the responses by using the transient method to simulate the forced response to a harmonic input until steady state is reached. In this case such an approach would be time consuming and challenging because the nonlinearities couple the modes, creating a steady-state response composed of many signals. Instead, the energy dissipation is calculated using the analytical formulas derived in [3], which develop distinct expressions for energy dissipation in micro-slip and macro-slip. The analytical energy dissipation values are converted to a damping values via Eq. (9).

5.2. SDOF Comparison Results

Using the values for the Jenkins element parameters defined previously, both the Stuttgart and Imperial approaches calculated damping values for their respective nonlinear elements at excitation force amplitudes of 20 N, 30 N, 50 N, and 70 N. The resulting damping values of both the Jenkins element and the 3D contact element are identical, as expected, because the 3D contact element reduces to a Jenkins element when applied to only one dimension. The parameters for the Iwan element were adjusted until the analytical damping curves aligned as closely as possible with those of the Jenkins element.

Figure 11 compares the final Iwan element analytical curves for effective critical damping ratio versus displacement amplitude with the calculated damping versus amplitude for the Jenkins element. The following parameters were used for the Iwan model: $F_S = 2.5$ N, $K_T = 20000$ N/mm, $\chi = -0.5$, and $\beta = 0.5$. The comparison illustrates that a single Jenkins element exhibits power-law energy dissipation with a slope of -1 on a log-log damping versus amplitude plot, and to mimic this behaviour the Iwan element must be in the macro-slip regime. The micro-slip parameter of the Iwan element, χ, controls the shape of the left half of the curve and, hence, is irrelevant for this comparison.

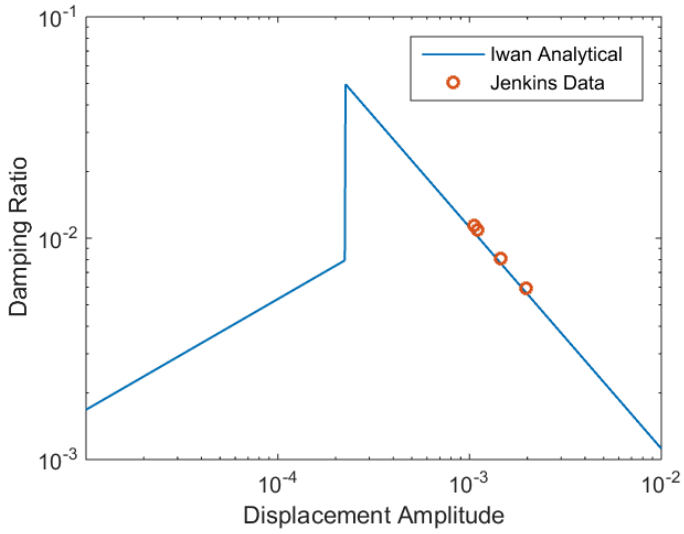

Figure 11: Comparison of damping vs. amplitude behaviour of a single Jenkins element in the SDOF system shown in Fig. 10 with that of an Iwan element.

Of course, this simple example does not really illustrate the intended regime that will likely be observed in the Brake-Reuss beam, micro-slip, where some of the Jenkins elements remain stuck while others slip. The net effect of all of those Jenkins

elements is expected to produce power law energy dissipation with a slope greater than zero on a plot similar to that shown in Fig. 11. In the micro-slip regime, the parameters for the Iwan element can presumably be adjusted until its behaviour matches the observed behaviour.

6. BRAKE-REUSS BEAM NONLINEAR DYNAMIC ANLAYSIS

6.1. Reduced Interface Frequency Response Analysis

The two harmonic balance approaches, those used at Stuttgart and Imperial, performed a preliminary nonlinear dynamic analysis on the Brake-Reuss beam by applying their nonlinear elements on a smaller portion of the full contact interface. The specific nodes that are activated for this "reduced interface" analysis are those highlighted in Fig. 12, which consist of the nodes inside the 0.688-inch diameter circular areas surrounding the holes. Each node is tied to its coincident node belonging to the opposite surface with a nonlinear element.

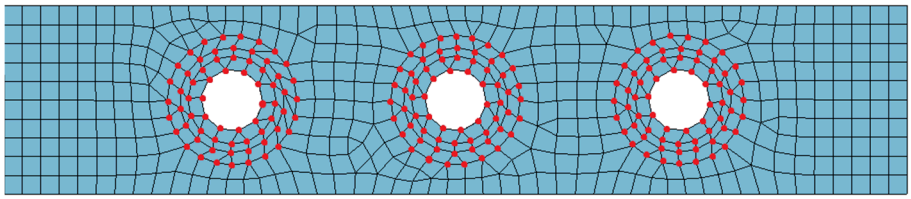

Figure 12: The activated nonlinear nodes in the reduced interface dynamic simulations.

The finite element conditions of the beam are the same as described in Section 2.1. In addition, a force acting in the x-direction is applied on a corner node at the opposite end of the structure from the fixed end, as shown in Fig. 13. This same driving node is also chosen as the output node for the x-direction response. A static pre-tension load of 4 kN is applied for each of the bolts to model the bolt compression on the joint. The simulations were conducted for input force magnitudes of 1 N, 10 N, 20 N, 50 N, 100 N, and 200 N between a frequency range of 150 Hz and 180 Hz in order to capture the 2nd bending mode of the Brake-Reuss beam.

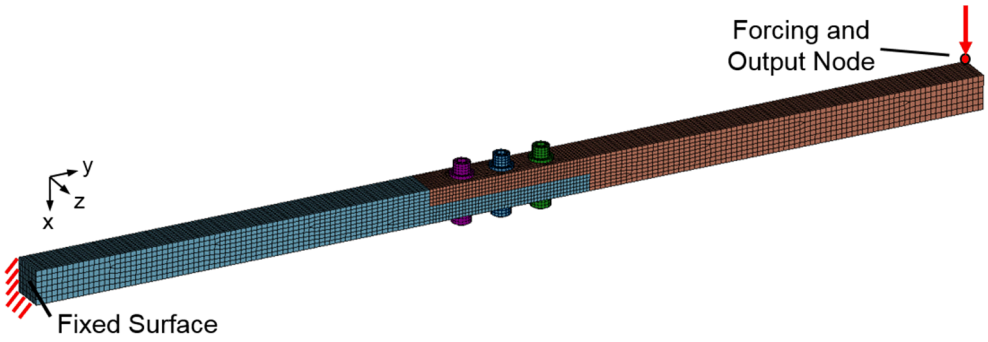

Figure 13: Finite element nodal definitions for the reduced interface simulations.

Figure 14 shows the nonlinear frequency response (FRF) curves estimated by Stuttgart's approach (Jenkins element) for all six simulated excitation levels. The response curves are normalized by the input force magnitude to better illustrate how the resonance peaks change shape as the force magnitude is increased. These results show the expected behaviour for a joint in that, as the forcing magnitude increases, more elements change their contact states to slip and therefore decrease the resonance frequency. The shrinking and widening of the peaks implies an increase in the effective damping. Figure 14 also shows the linear FRFs for the elastic cases when all the Jenkins elements are stuck (effectively acting as linear springs), and when they are all slipping (zero spring behaviour), representing the two extremes of the dynamic behaviour of the two jointed beams.

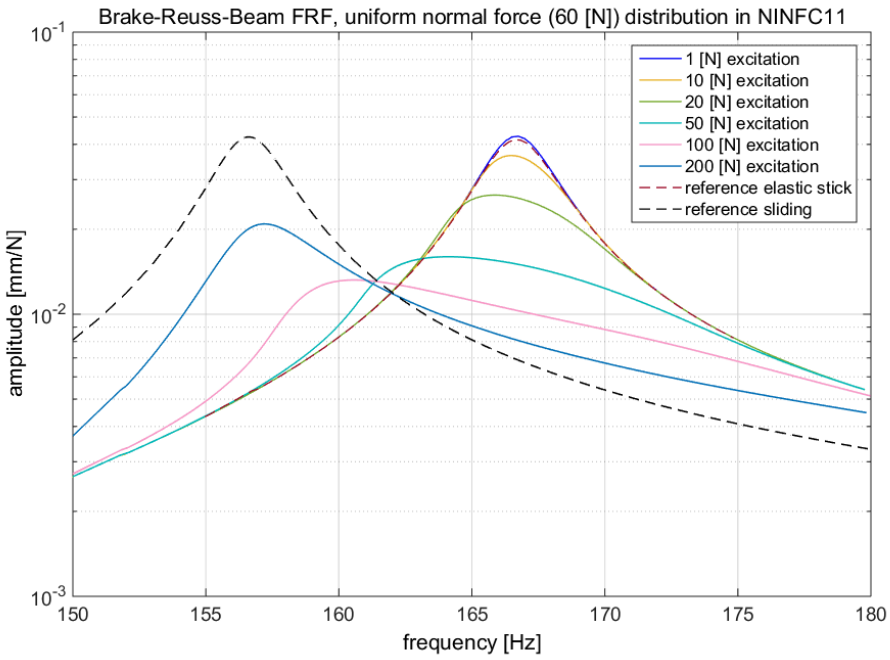

Figure 14: Stuttgart's frequency response prediction for the reduced interface model.

Figure 15 shows the FRF obtained by the Imperial with the 3D contact nonlinear elements. For the smaller excitations the change in frequency and damping behaviour is quite similar to Stuttgart's responses, however several differences can be observed at higher excitation levels. Imperial's model allows a relative displacement in surface normal direction, and therefore allows variations in the contact normal forces as well as lift-off phenomena, which are increased by higher excitation amplitudes. These effects can reduce the magnitude of relative displacement in tangential directions and therefore result in less dissipation and sliding of contact elements.

The observation that lift-off phenomena and contact normal force variation play a considerable role even for the reduced contact interface motivated the authors to investigate the dissipative behaviour of the beam structure considering the entire interface.

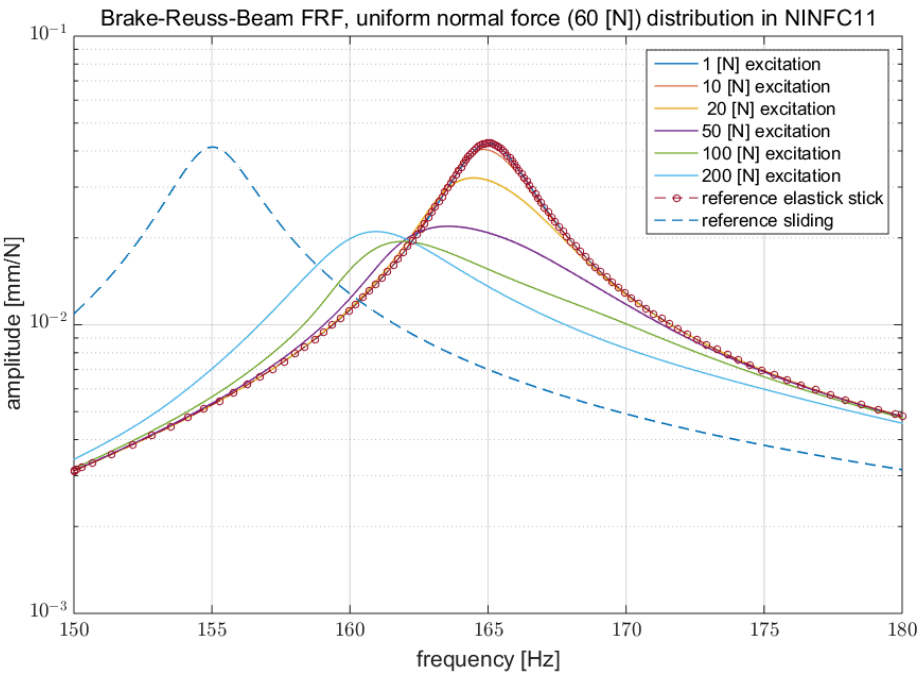

Figure 15: Imperial's frequency response prediction for the reduced model.

6.2. Full Interface Analysis

Following the reduced interface analysis, another analysis is conducted involving all three approaches in which all the nodes over the entire contact interface are considered for coupling with nonlinear elements. Stuttgart's model assigned the interpolated contact normal forces to individual nodes based on the previous nonlinear static analysis (Fig. 5). Only the 460 statically loaded nodes, seen in Fig. 16, are activated under the assumption that the contact state in normal direction would not change for the dynamic analysis. Imperial's model, on the other hand, activates all 592 nodes on the contact interface for coupling with 3D contact elements to their coincident counterparts.

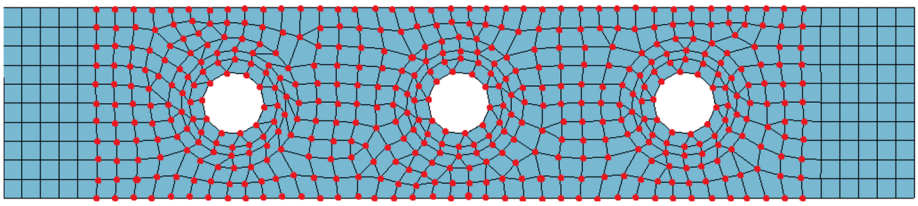

Figure 16: The active nodes used in Stuttgart's full interface model.

The nodal definitions for the Brake-Reuss beam finite element model are altered slightly from the reduced interface analysis in an attempt to reproduce the experimental testing being done on the beam in parallel with this analysis. As seen in Fig. 17, the input force location is moved to the opposite surface of the beam to act in the x-direction at a point 18.922 inches away from the fixed end of the beam (the location of a threaded hole in Fig. 1). Likewise, the output node is moved to another corner at the free end of the beam, but the x-direction response is still desired. The same 4 kN static pre-load is applied on the bolts, and simulations are conducted for input force magnitudes of 1 N, 10 N, 50 N, and 100 N for a frequency range between 150 Hz and 190 Hz.

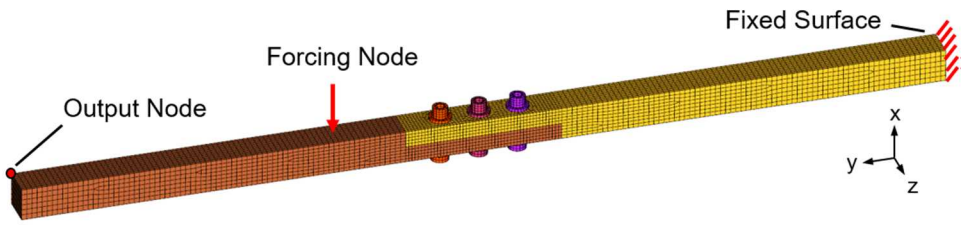

Figure 17: Finite element nodal definitions for the harmonic balance full interface simulations.

The resulting 2nd bending resonance frequency shift for both the Imperial and Stuttgart models is plotted in with increasing excitation force in Fig. 18. As expected, the resonance frequency decreases as the input force magnitude increases. Comparing these frequencies with the peak locations of the nonlinear FRFs from the reduced interface analysis (Section 6.1), both full interface models have a notable 15 Hz resonance frequency increase for small amplitude excitation. This is also expected as extending nonlinear elements to more of the interface increases the joint stiffness due to more coupling between nodes along the length of the beam.

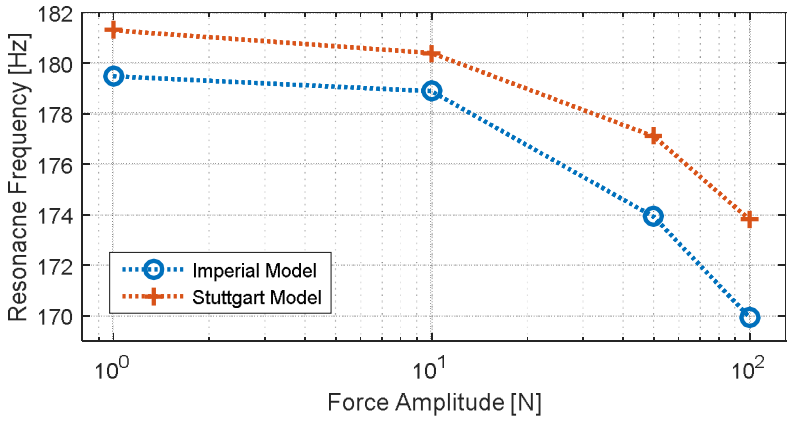

Figure 18: Finite element nodal definitions for the harmonic balance full interface simulations.

With its capability to simulate having nonlinear elements at all nodes on the interface, another analysis is performed on the Imperial model to examine the slip state of the elements at resonance for the 1st bending mode. Figure 19 shows the resulting slip states. It is interesting to note how there is a region surrounding the middle hole where the elements do not experience slipping. For the other regions, the boundary where the contact surfaces separate at some point in the resonance cycle is consistent with the shape of the static pressure distribution and gap shown in Fig. 5.

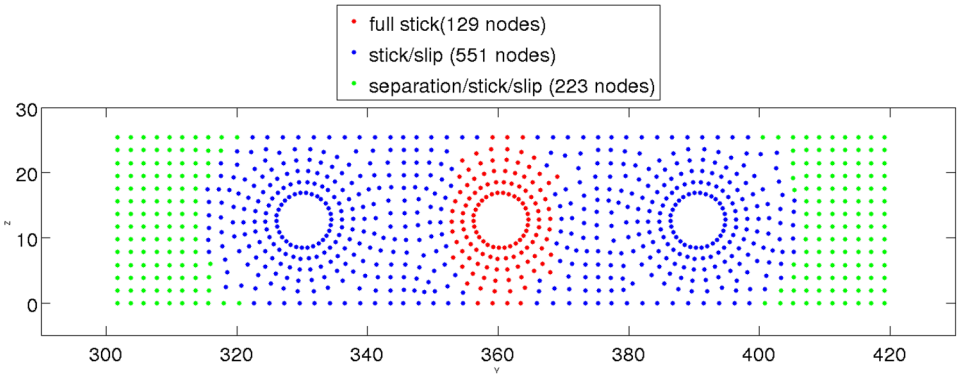

Figure 19: The slip-stick contact conditions for the nonlinear elements in Imperial's model at resonance for the 1st bending mode.

6.3. Tuning the Iwan Element Joint Model Using Amplitude-Dependent Damping

When observing the effect that the presence of a joint has on a structure, the typical quantities of interest are how both the resonance frequency and the energy dissipation (or critical damping ratio) for a particular vibration mode changes as the structure is excited with larger excitation forces. This opens a route for comparison between transient and harmonic responses because there exist methods to extract these two quantities from either type of response. Other works have shown that one can obtain insight into the joint dynamics by plotting energy dissipation versus the amplitude of either the response or the force in the joint, and that dissipation tends to follow a power-law relationship [6]. If power-law relationships can be established for the energy dissipated by the Jenkins and 3D contact elements, then the four-parameter Iwan model may be tuned to match those relationships.

For both of the harmonic approaches, the energy dissipated is calculated as described in Section 5.1 for Imperial's approach. In effect, the hysteresis curves for each nonlinear element can be constructed at resonance, and the total energy dissipated is the sum of the areas of all the hysteresis curves. If the energy dissipation follows a power-law relationship with an exponent of χ+3, then damping ratio will also follow a power-law with an exponent χ+1 because the damping ratio is related to dissipation via Eq. 9, in which dissipation is divided by a power 2 term in the denominator. A plot of the damping versus amplitude on a logarithmic scale for the two harmonic balance approaches is shown in Fig. 20. The data for each approach are from the four nonlinear frequency response simulations calculated under the conditions described in Section 6.2. Note that the velocity amplitude is taken from the linear mode shape of the 2nd bending mode, which might contaminate the obtained results and explain the deviations because the real shape is a superposition of the kept ROM modes which are coupled by nonlinear forces.

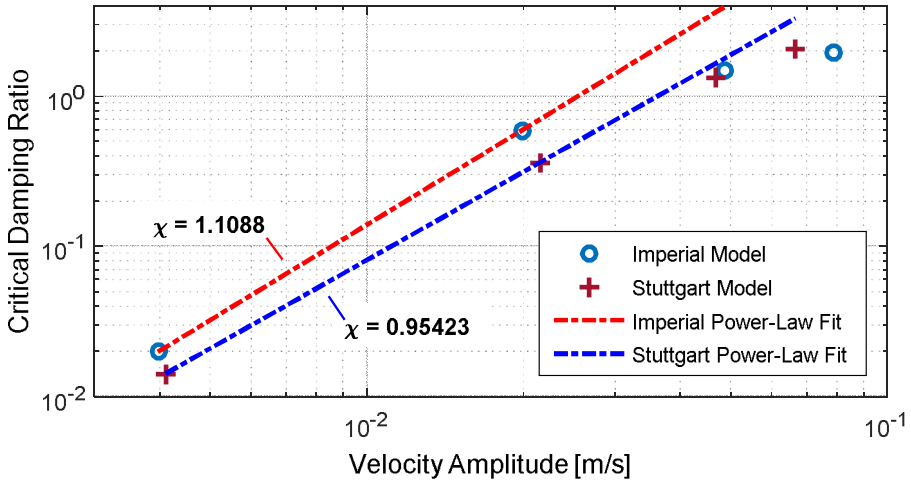

Figure 20: Damping ratio versus beam tip velocity amplitude for the second mode (near 178 Hz) predicted by each method.

The results seem to show that both the Stuttgart and Imperial codes predict that this mode's damping will follow a power-law relationship at low amplitudes, but then at higher amplitudes the damping begins to level off, presumably as the system approaches macro-slip. The dashed lines correspond to a power-law fit to the damping versus amplitude of the following form,

$$\zeta_r = C_r |V_r|^{\chi+1}. \tag{10}$$

Imperial's model has a power law strength of $C_r = 2300$ while Stuttgart's is $C_r = 656$. Both have relatively similar power-law exponents, $\chi = 1.10$ for Imperial and $\chi = 0.95$ for Stuttgart. It is interesting to note that in previous works χ has typically been found to have values near -0.3 (see, [6] or [7]). Here χ is positive and near 1.0 so damping is growing with the second power of the velocity amplitude. As a result, the damping measured in a low amplitude test would quickly become erroneous as amplitude increases. On the other hand, it appears that the system only follows a power-law relationship over a relatively small range of amplitude, and then it seems to transition to macro-slip.

In principle, one could use the power law fit above to fit a modal Iwan model [17,18] to this damping vs. amplitude behaviour. One could then predict the response of this mode in the micro-slip regime using the SDOF equation of motion for

the modal Iwan model at a low computational cost. However, the power law coefficients, C_r, above are quite large. An Iwan model with $\chi = 1.10$ and $R = 1.591\times10^{17}$ would reproduce the power-law fit above, but since (from [3])

$$R = \frac{K_T^{\chi+2}(\chi+1)\left(\beta+\frac{\chi+1}{\chi+2}\right)^{\chi+1}}{F_S^{\chi+1}(1+\beta)^{\chi+2}} \tag{11}$$

and hence $R \approx K_T^{\chi+2}/F_S^{\chi+1}$, or $1.591\times10^{17} = K_T^{3.1}/F_S^{2.1}$, the stiffness of the joint, K_T,will have to be much higher than the slip force, F_S, for this is to be realized. The joint stiffness governs the shift in the resonance frequency as the joint goes from micro to macro-slip, and the resonance frequency of this mode decreases only to 155 Hz (a reduction of 25 Hz) if the joint stiffness goes to zero. Hence, the large K_T value that this demands is physically unreasonable. This discussion pertains only to Segalman's four-parameter Iwan model [3]. An alternative model, such as Mignolet's 5-parameter model [19] might have the flexibility needed to describe this behaviour.

It is also interesting to ask whether a finite element model with discrete Iwan elements at the locations of the bolts, such as the models that were advocated in [6], might reproduce the response of this structure. In [6] it was presumed that experiments could be performed on each joint in isolation to deduce their Iwan parameters, but no such experiments are available for this analysis. One could, instead, postulate a set of Iwan parameters and adjust them until simulations of the structure's response reproduce the desired damping versus amplitude behaviour. This was pursued by creating a reduced-order model of the Brake-Reuss beam as follows.

Since the Iwan element is a whole-joint model, it is counter to its intended use to define several hundred node parings over the joint interface to be coupled with the elements, as is done for the other approaches. Instead, the nodes on the interface are divided into three regions, and all the nodes within each region are tied to a representative virtual node with element spiders, as illustrated in Fig. 21. The element spiders are defined as NASTRAN RBE3 elements [9], which are interpolation elements that force the motion of the virtual node to be a weighted average of the motion of the tied nodes on the surface. The same virtual node and RBE3 specification is defined for the opposite surface.

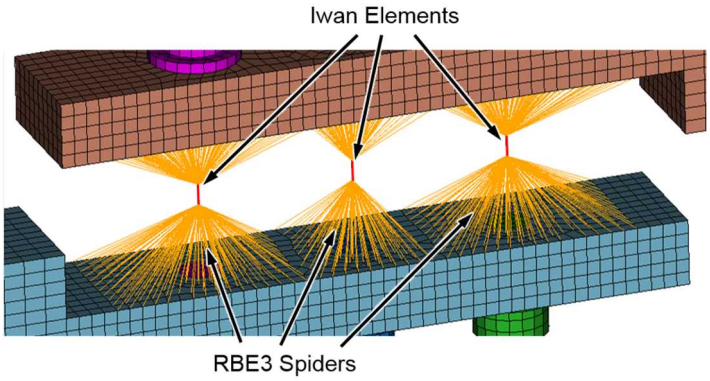

Figure 21: The Sandia joint model for the full interface analysis. The interface shown in an exploded view.

The three virtual node pairs, the output point shown in Fig. 16, and the fixed surface nodes are selected as boundary nodes for Craig-Bampton reduction [10]. The first 21 fixed-interface modes are kept to ensure that the model is accurate up to at least 4000 Hz, though such detail in the response may be unnecessary. Post-reduction, the out-of-plane rotational degrees of freedom between virtual node pairs are constrained to move with each other. In addition, each virtual node pair is coupled with two Iwan elements, one for each surface tangent direction. With three virtual node parings, there are six total Iwan elements in the Sandia joint model.

Since the parameterization for each Iwan element is unknown, they are all assumed to have the same parameter values. The slip force F_S is set to 2400 N, and the joint stiffness K_T is set to 10^7 N/mm, a minimum value that produces the same resonance frequency for the 2nd bending mode as the harmonic approaches when all the joints are completely stuck. The value for β is held constant at 0.05, and χ is left as a variable to observe how it affects the calculated damping.

Material damping is added to the structure by transforming a diagonal matrix of modal damping ratios ζ_m obtained from previous experiments into the damping coefficient matrix $\hat{\mathbf{C}}$ in the Craig-Bampton space. This is done through

$$\hat{\mathbf{C}} = \hat{\mathbf{M}}\boldsymbol{\Phi} \cdot diag(2\omega_r\zeta_m) \cdot \boldsymbol{\Phi}^{\mathrm{T}}\hat{\mathbf{M}}, \tag{12}$$

where $\boldsymbol{\Phi}$ is the matrix of mass-normalized mode shapes $\boldsymbol{\phi}_r$ produced from the Eigen analysis of

$$\left(\hat{\mathbf{K}} - \lambda_r\hat{\mathbf{M}}\right)\boldsymbol{\phi}_r = \mathbf{0}. \tag{13}$$

$\hat{\mathbf{M}}$ is the Craig-Bampton-reduced mass matrix, $\hat{\mathbf{K}}$ is the reduced stiffness matrix that includes the full stick joint stiffness contribution, and $\omega_r = \sqrt{\lambda_r}$ are the circular resonance frequencies. The modal damping ratios for the 1st and 2nd bending modes are 0.008 and 0.0051, respectively.

In transient methods, the instantaneous nonlinear damping can be retrieved from the free-response signal using the Hilbert transform methods outlined in [8]. The 2nd bending mode of the beam is excited by applying a force in the shape of the mode as follows,

$$\mathbf{f}_{ext} = p\hat{\mathbf{M}}\boldsymbol{\phi}_2 \tag{14}$$

Where $\boldsymbol{\phi}_2$ is the mode shape for the 2nd bending mode, and p is a scalar for the force magnitude. Several transient simulations were performed with an impulsive input in the shape of one cycle of a sine with period of 5.59 ms (2nd bending mode period) and amplitude $p = 5000$. The transient response was found by integrating the equations of motion, including the six Iwan joints, using the Newmark routine with a time step between 1 and 10 microseconds. The reduced model had 54 degrees of freedom and about 30 minutes were required to find the response at the approximately 2 million time steps that were needed for the transient signal to decay. These simulations were on a desktop computer with a 3-GHz quad-core processor; though only one of the cores was utilized by the Newmark routine. Relatively little effort was exerted to find the optimal time step or to minimize the size of the Craig Bampton model, so these simulation times could probably be improved.

Figure 22 shows how the frequency and damping of the mode in question varies as χ is adjusted. More negative values of χ produce higher dissipation (for fixed values of F_S and K_T), and a larger shift in the resonance frequency with amplitude. All of these simulations remained in the micro-slip regime. Note that, in contrast to the results shown in Fig. 20, the damping ratio shown includes contributions from both the material damping and the damping due to the joint. As a result, the curves do not seem to show power-law behaviour but instead converge to a low amplitude asymptote (the material damping, which is 0.0051).

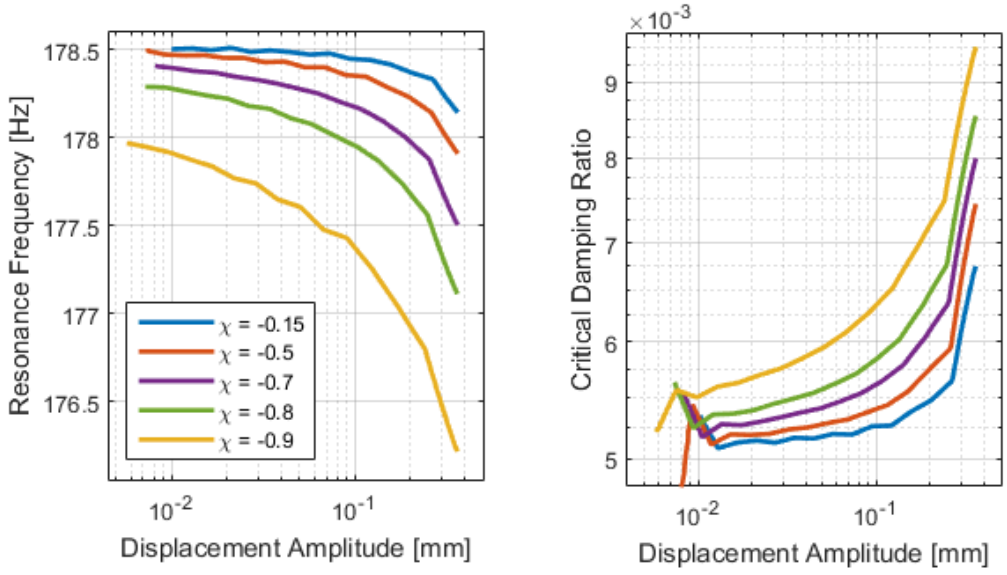

Figure 22: Frequency and damping versus displacement amplitude at the tip for various models with discrete Iwan joints.

It is also interesting to note that the χ value used for the discrete joints does not end up having the same χ value that best fits the modal damping versus displacement curves. For example, for the case where χ = -0.9, a power-law model was fit and the parameters found were χ = -0.27 and C_r = 0.00472. This power-law strength, C_r, is far lower than what is predicted by the Imperial and Stuttgart approaches, so the parameters of the discrete Iwan joints would have to be adjusted significantly to match that behaviour. Even so, it is probably not possible to obtain agreement for this mode using a 4-parameter Iwan model for the joints.

7. CONCLUSION

This project investigates three modelling approaches on their ability to model the dynamic behaviour exerted by a bolted joint in a structure. In the course of completing the analyses described in previous sections, a number of conclusions and lessons learned are gained regarding the optimal use of each approach and their nonlinear elements.

If using nonlinear elements similar to the Jenkins and 3D contact elements, which describe binary stick-slip behavior in a very localized region of the friction interface, then effort must be made to model many such elements distributed over most, if not the entire, interface. As is shown in Section 5.2, using a single Jenkins or 3D contact element would capture macro-slip behaviour of a joint, but not the essential micro-slip behaviour that simulates the small-amplitude response produced in bolted lap joint structures. In addition, Section 6.2 shows that spreading nonlinear contact elements over the entire interface may capture the resonant frequencies in a structure more accurately than over reduced regions in the interface.

One advantage to developing models that spread many nonlinear elements over the joint interface is that the analyst can gain a detailed picture on the state of the localized regions in the interface while the joint is in motion. Such a picture is demonstrated in Fig. 19, which summarizes the stick-slip-separation states for the 3D contact elements at all nodes on the interface within one cycle of the Brake-Reuss beam's first bending mode. The ability to observe local states can be useful for analysts interested in the elastic dynamics inside the joint interface.

The downside to adding tens or hundreds of nonlinear elements in the interface is that they strain the convergence rate in implicit transient solvers. If convergence is possible, the time step required may be so small as to require weeks or months of computation to simulate a useful amount of response history. Such a time investment is not practical from a design standpoint, and the analyst would need to rely on more efficient methods for retrieving the response, like the harmonic balance method. In using the harmonic balance method, the analyst is restricted to oscillatory inputs. Of course, this is not a problem if the forced harmonic response is desired, and the harmonic balance method is recommended for its efficiency in these cases provided that the influence of the nonlinear element can be represented somehow in the frequency domain.

An alternative for many stick-slip elements is a single whole-joint formulation, such as the Iwan element, that in itself describes the local stick-slip distribution needed to model micro-slip. A finite element model would only require at most a few whole-joint models, which restores the practicality for numerical time integration schemes. In return, the whole-joint modelling methods used in this research require rigid element spiders or averaging MPCs to couple the joint interfaces, which potentially add artificial stiffness to the joint and may adversely alter the structure's resonance frequencies. In addition, whole-joint elements may not carry the same level of detailed contact states shown by many individual stick-slip elements. As such whole-joint models like the Iwan element are recommended if the influence that the joint has on the rest of the structure is of greater interest than the dynamics occurring within the joint itself.

This research shows that harmonic and transient responses can be linked for comparison by observing how a structure's resonant frequencies and nonlinear damping changes with response amplitude. In Section 6.3, the damping versus amplitude power-law relationships from the two harmonic balance models are used to try and parameterize the Iwan joint to reproduce their energy dissipation behaviours. This approach did not succeed as well as hoped. Nonetheless, the dynamic response output from the harmonic balance approaches is recast in a way that shows that their power-law exponents apparently exceed those seen in experiments on some jointed structures, and that it is difficult for the four-parameter Iwan model to reproduce that behavior. Further study would need to be conducted to determine the source of these anomalies and whether additional corrections are needed for a more fair tuning analysis.

Although much is gained from this research, it is still very much a work in progress, and a few next steps are recommended. For the Jenkins and 3D contact element models, (INSERT NEXT STEPS). With regards to the whole-joint Iwan models,

further study is needed to assess the effects that dividing the interface into fewer or more spider patches (even exchanging RBE3 spiders for rigid bar elements) has on the dynamic response of the Brake-Reuss beam. All models, of course, also require a validation study with experimental data on the Brake-Reuss beam. Such a study will also facilitate a more meaningful comparison between the transient and harmonic balance methods, since all models will work to simulate the same, real structure.

ACKNOWLEDGEMENTS

The authors would like to thank Sandia National Laboratories for supporting this research during the 2015 Sandia Nonlinear Mechanics and Dynamics Summer Research Institute. Special thanks is given to Professor Matthew Allen at the University of Wisconsin-Madison for his insights on the use of Iwan models in numerical simulation, and for his guidance in the analysis of the dynamic response results to compare their modal damping behaviours. Thanks is given to Dr. Timothy Truster from the University of Tennessee for his suggestions on the directed course of this research during the latter half of the Institute.

REFERENCES

[1] Salles, L., Swacek, C., Lacayo, R.M., Reuss, P., Brake, M.R.W., and Schwingshackl, C.W., 2015, "Numerical Round Robin for Prediction of Dissipation in Lap Joints," In *IMAC XXXIII A Conference and Exposition on Structural Dynamics*, Orlando, FL.

[2] Brake, M. R., Reuss, P., Segalman, D.J., and Gaul, L., 2014, "Variability and Repeatability of Jointed Structures with Frictional Interfaces," In *IMAC XXXII A Conference and Exposition on Structural Dynamics*, Orlando, FL.

[3] Segalman, D.J., 2005, "A Four-Parameter Iwan Model for Lap-Type Joints," *ASME Journal of Applied Mechanics*, **72**, pp. 752-760.

[4] Iwan, W.D., 1966, "A Distributed-Element Model for Hysteresis and its Steady-State Dynamic Response," *ASME Journal of Applied Mechanics*, **33**(4), pp. 893-900.

[5] Smallwood, D.O., Gregory, D.L., and Coleman, R.G., 2000, "Damping Investigations of a Simplified Frictional Shear Joint," *SAND2000-1929C*, Sandia National Laboratories, Albuquerque, NM.

[6] Segalman, D.J., Gregory, D.L., Starr, M.J., Resor, B.R., Jew, M.D., Lauffer, J.P., and Ames, N.M., 2009, *Handbook on the Dynamics of Jointed Structures,* Sandia National Laboratories, Albuquerque, NM.

[7] Deaner, B.J., Allen, M.S., Starr, M.J., Segalman, D.J., and Sumali, H., 2015, "Application of Viscous and Iwan Modal Damping Models to Experimental Measurements from Bolted Structures," *ASME Journal of Vibration and Acoustics*, **137**(2), 021012.

[8] Roettgen, D.R., and Allen, M.S., 2015, "Nonlinear Characterization of a Bolted, Industrial Structure Using a Modal Framework," *Mechanical Systems and Signal Processing*, submitted June 2015.

[9] Reese, G., Segalman, D., Bhardwaj, M.K., Alvin, K., Driessen, B., Pierson, K., Walsh, T., Dohrmann, C., and Wilson, C.R., 2012, *Salinas-User's Notes*, Sandia National Laboratories, Albuquerque, NM.

[10] Bampton, M.C.C., and Craig, R.R., 1968, "Coupling of Substructures for Dynamic Analyses," *AIAA Journal*, **6**(7), pp. 1313-1319.

[11] Brake, M.R., 2013, "IMEX-a: An Adaptive, Fifth Order Implicit-Explicit Integration Scheme," *SAND2013-4299*, Sandia National Laboratories, Albuquerque, NM.

[12] Bograd, S., Reuss, P., Schmidt, A., Gaul, L., and Mayer, M., 2011, "Modeling the Dynamics of Mechanical Joints," *Mechanical Systems and Signal Processing*, **25**, pp. 2801-2826.

[13] Cigeroglu, E, Özgüven, H.N., 2006, "Nonlinear Vibration Analysis of Bladed Disks with Dry Friction Dampers," *Journal of Sound and Vibration,* **295**, pp. 1028-1043.

[14] Petrov, E.P., and Ewins, D.J., 2002, "Analytical formulation of friction interface elements for analysis of nonlinear multiharmonic vibrations of bladed discs," *ASME Journal of Turbomachinery*, **125**, pp. 364-371.

[15] Petrov, E.P., and Ewins, D.J., 2004, "Generic Friction Models for Time-Domain Vibration Analysis of Bladed Disks," *ASME Journal of Turbomachinery*, **126**, pp. 184-92.

[16] Petrov, E.P., 2011, "A High-Accuracy Model Reduction for Analysis of Nonlinear Vibrations in Structures with Contact Interfaces", *Transactions of the ASME: Journal of Engineering for Gas Turbines and Power*, **133**, 102503.

[17] Segalman, D.J., 2010, "A Modal Approach to Modeling Spatially Distributed Vibration Energy Dissipation," *SAND2010-4763*, Sandia National Laboratories, Albuquerque, NM.

[18] Deaner, B.J., 2013, "Modeling the Nonlinear Damping of Jointed Structures using Modal Models," M.S., Engineering Physics, University of Wisconsin-Madison, Madison, WI.

[19] Mignolet, M.P., Song, P., and Wang, X.Q., 2015, "A Stochastic Iwan-Type Model for Joint Behaviour Variability Modeling," *Journal of Sound and Vibration*, **349**, pp. 289-298.